A PRIORI ERROR ESTIMATES FOR LOCAL RELIABILITY-BASED SENSITIVITY ANALYSIS WITH MONTE CARLO SIMULATION

A.J. TORII AND A.A. NOVOTNY

ABSTRACT. In this work, we present *a priori* error estimates for local reliability-based sensitivity analysis. The Score Function Method and the Weak Approach using Monte Carlo Simulation are studied. The results are important for practical choice of parameters in local sensitivity analysis. Besides, the results can be employed for development of *a posteriori* error estimates and adaptive schemes in the future. The theoretical results are obtained for the one dimensional case, but are also useful in the multidimensional context, as confirmed through a set of numerical experiments.

1. INTRODUCTION

Probabilistic sensitivity analysis measures the influence of model inputs into probabilistic outputs. Sensitivity analysis can be broadly classified according to three criteria: scope (global vs local), quantity of interest (e.g. expected performance, variance, probability of failure, quantiles) and methods (e.g. sampling-based schemes, stochastic expansion, surrogate models, dimension reduction). Local sensitivity analysis evaluates the influence of deterministic model parameters into quantities of interest. This is generally done by evaluation of partial derivatives. Global sensitivity analysis (GSA), on the other hand, measures the influence of random model parameters into quantities of interest. Sensitivity indexes, such as Sobol's indexes, are generally employed for this purpose.

Reliability-based sensitivity analysis is of paramount importance for several fields, such as uncertainty based design, decision under uncertainties, uncertainty based optimization, model building and calibration, among others. For this reason, sensitivity analysis has been intensively studied in the last decades. Some recent advances involve application of GSA to vehicle crash simulation [33], development of Kullback-Leibler divergence based GSA and its application to offshore wind turbines [43], development of Kriging based GSA approaches [7, 14], development of Line Sampling schemes for local reliability-based sensitivity analysis [46, 47], development of GSA based on Fréchet derivative [8], development of quantile based GSA [20, 17], development of GSA for multivariate outputs [24] and dynamic models [52], application of dimensional reduction to GSA [51, 23], converge studies regarding Morris' extension methods for GSA [5], GSA using orthogonal augmented radial basis function [48], GSA in the presence of multi-uncertainty [11], application of GSA to urban drainage simulation using principal component analysis and sparse Polynomial Chaos Expansion (PCE) [30], development of theoretical framework for time-dependent variance based GSA [1], stochastic collocation for GSA for medium-dimensional structural engineering problems [15], development of saddle-point approximation for dynamic systems reliability and local reliability-based sensitivity analysis [54], GSA in high dimensions with partial least squares PCE [12], benchmark problems for GSA [6], conceptual improvements concerning variance based GSA [25] and literature reviews [2], among others.

In this work, we address local reliability-based sensitivity analysis, i.e. the influence of deterministic model parameters into the probability of failure. In local sensitivity analysis of

Key words and phrases. probability of failure, reliability, sensitivity analysis, error estimate.

probability of failure, we evaluate the derivatives of the probability of failure with respect to design parameters [35, 21, 13, 45, 31, 44]. This is an important subject for risk and reliability-based design, since the sensitivities can be employed to guide the design procedure. Besides, the derivatives are required if gradient based optimization algorithms are applied for this task, as occurs in Risk and Reliability-Based Design Optimization.

The main difficulty concerning probability of failure sensitivity analysis is that evaluation of the probability of failure is generally a computationally demanding problem by itself. Consequently, accurate evaluation of sensitivities frequently lead to very high computational costs. For this reason, development of new methods and improvement of existing ones is a topic of intensive research. In the last decades, most advances were achieved by employing efficient methods for evaluation of the probability of failure, such as Line Sampling [46, 47, 27], Subset Simulation [4, 42], Kriging based Importance Sampling [10], Stochastic Expansion [45], Adaptive Importance Sampling [31], Subdomain Sampling [50], Moving Particles Methods [32], to cite a few. A rich literature review concerning local reliability-based sensitivity analysis can be found in the recent works [50, 32].

Local sensitivity analysis of probability of failure can be divided into two mains cases, depending whether the design parameter affects the distribution of the random variables or the limit state function. The methods frequently employed for each case are summarized in Table 1. The Score Function Method [35, 40, 38, 19] is the standard approach when the design parameter affects the distribution of the random variables, since the estimate is unbiased, as discussed in Section 3. Three approaches are commonly adopted when the design parameter affects the limit state function. The Direct Approach follows from a direct application of Finite Difference Formulas. The Common Random Variable (CRV) approach is also based on Finite Difference Schemes, but the sample is not redrawn during evaluation of the Finite Difference Formula [19], a measure that is known to reduce the variance of the estimate [44]. The Weak Approach, on the other hand, is based on an approximation for the weak derivative of the probability of failure [21, 45].

Table 1. Approaches for local probability of failure sensitivity

Design parameter affects	
Random Variables	Limit State Function
Score Function Method	Direct
	Common Random Variable (CRV)
	Weak

A priori error estimates for probability of failure sensitivity analysis using Monte Carlo Simulation (MCS) were presented in [44]. The Weak, the Direct and the CRV approaches were studied. It was demonstrated that the root mean square (rms) error of the estimate depends not only on the probability of failure but also on its derivatives, a result that was intuitively anticipated in [31]. However, in [44] only the case where the design parameter does not affect the random variables was addressed. Besides, the bias estimate obtained for the Weak Approach considered a single random variable and was not representative for more general situations. The main goal of the present work is to fill these two gaps.

In this work, we derive *a priori* error estimates for the Score Function Method and the Weak Approach, given by Eqs. (3.12) and (3.28), respectively. The bias estimate for the Weak Approach presented here has been observed to be more representative than that obtained in the work [44]. These results fill the two main gaps from the work [44]. The CRV with Central Formula is also discussed because of its theoretical similarity to the Weak Approach. The CRV

with Forward Formula and the Direct Approach were not further studied in this work (see [44] for more details on these approaches).

Note that general purpose error estimates for the Score Function Method are known for some time. In fact, the works [38, 39] presented error estimates that hold for expectations in general, derivatives of arbitrary order and consider employment of Importance Sampling. In this work, we rather focus on the particular case of error estimates concerning derivatives of the probability of failure. Thus, the result from Eq. (3.7) is actually a particular case of the estimates presented in [38, 39]. The results from Eq. (3.12), on the other hand, are novel.

The error estimates presented here were obtained for MCS [38, 19, 36]. The choice for MCS is based on two main reasons. First, most sampling-based schemes share common aspects with MCS. We thus expect that the error estimates presented in this work may be adapted for more advanced sampling based-schemes in the future. Second, MCS is likely the most popular sampling scheme for problems that do not involve high computational costs. Consequently, the results presented here are valuable for a wide range of applications.

The rest of this paper is organized as follows. In Section 2, we present a brief review of probability of failure sensitivity analysis. The error estimates obtained in this work are presented in Section 3, where we also demonstrate how the derived results can be employed for optimal choice of parameters. Numerical examples that validate the obtained results are presented in Section 4. The main conclusions of this work are summarized in Section 5. Additional results are presented in the Appendices.

2. Probability of failure sensitivity

Let us consider that $g(\mathbf{X}, \rho)$ is a limit state function depending on a design parameter $\rho \in \mathbb{R}$ and a random vector $\mathbf{X} \in \mathbb{R}^d$, $d \geq 1$, with probability density function $f_{\mathbf{X}}$ [18, 26, 41, 37]. The probability of failure can then be defined as [28, 9, 29]

$$\begin{aligned} P_f(\rho) &= \mathbb{P}[g(\mathbf{X}, \rho) < 0] \\ &= \int_{\Omega} I(g(\mathbf{x}, \rho)) f_{\mathbf{X}}(\mathbf{x}) d\mathbf{x} \\ &= \mathbb{E}[I(g(\mathbf{X}, \rho))], \end{aligned} \tag{2.1}$$

where $\mathbf{x}$ represents a realization of the random vector $\mathbf{X}$, $\mathbb{P}$ indicates the probability of occurrence of a given event, $\mathbb{E}$ represents the expected value, $f_{\mathbf{X}}$ has support $\Omega \subset \mathbb{R}^d$ and I is the indicator function, namely

$$I(t) = \begin{cases} 1, & t < 0, \\ 0, & t \geq 0. \end{cases} \tag{2.2}$$

Here we consider the sensitivity

$$P_f'(\rho) = \frac{dP_f(\rho)}{d\rho}, \tag{2.3}$$

where the notation $(\cdot)'$ is employed throughout the text to represent the derivative of $(\cdot)$ with respect to the design parameter ρ. Sensitivity of P_f with respect to a design parameter that affects $f_{\mathbf{X}}$ can be addressed by the Score Function Method [35, 45, 40, 38]. If ρ does not affect the distribution $f_{\mathbf{X}}$, then the Weak, the Direct and the CRV approaches described in [44] can be employed.

2.1. **Score Function Method.** The Score Function Method can be employed when the design parameter only affects the distribution $f_{\mathbf{X}}$, i.e. when the limit state function g does not depend explicitly on ρ. In this case, direct differentiation of Eq. (2.1) with respect to ρ gives (see [35, 45, 40, 38, 19] for further details)

$$\begin{aligned}\overline{P}'_f(\rho) &= \mathbb{E}[I(g(\mathbf{X},\rho))s(\mathbf{X})] \\ &= \int_\Omega I(g(\mathbf{x},\rho))s(\mathbf{x})f_{\mathbf{X}}(\mathbf{x})d\mathbf{x},\end{aligned} \tag{2.4}$$

where s is the score function given by

$$s(\mathbf{x}) = \frac{1}{f_{\mathbf{x}}(\mathbf{x})}\frac{df_{\mathbf{x}}(\mathbf{x})}{d\rho}. \tag{2.5}$$

If the above sensitivity is evaluated with MCS we have the estimate

$$\hat{P}'_f(\rho) = \frac{1}{N}\sum_{i=1}^{N} I(g(\mathbf{x}_i,\rho))s(\mathbf{x}_i), \tag{2.6}$$

where N is the sample size and $\mathbf{x}_i$ are sample points.

The symbol $\overline{P}'_f$ is employed here to represent an approximation for P'_f. The symbol $\hat{P}'_f$, on the other hand, is employed to represent a MCS estimate for $\overline{P}'_f(\rho)$. In other words, $\overline{P}'_f(\rho)$ is the conceptual approximation for the sensitivity P'_f, whereas $\hat{P}'_f$ is the MCS estimate for $\overline{P}'_f(\rho)$. This notation is employed throughout the text. Latter we demonstrate that the Score Function Method is conceptually exact, apart from sampling errors.

2.2. **Weak Approach.** The Weak Approach can be employed when the design parameter ρ does not affect the distribution $f_{\mathbf{x}}$. In this case, we have (see [44] for further details)

$$\begin{aligned}P'_f(\rho) &= -\lim_{h\to 0}\mathbb{E}[\phi_h(g(\mathbf{X},\rho))g'(\mathbf{X},\rho)] \\ &= -\lim_{h\to 0}\int_\Omega \phi_h(g(\mathbf{x},\rho))g'(\mathbf{x},\rho)f_{\mathbf{x}}(\mathbf{x})d\mathbf{x},\end{aligned} \tag{2.7}$$

where ϕ_h converges to the Dirac delta function in the sense of distributions, for $h \to 0$. In this work we consider, without loss of generality, the following approximation

$$\phi_h(t) = \begin{cases} 0, & t < -h/2, \\ 1/h, & -h/2 \le t \le h/2, \\ 0, & t > h/2. \end{cases} \tag{2.8}$$

In practice, the above sensitivity is evaluated for sufficiently small h, thus giving the approximation

$$\overline{P}'_f(\rho) = -\mathbb{E}[\phi_h(g(\mathbf{X},\rho))g'(\mathbf{X},\rho)]. \tag{2.9}$$

The MCS estimate results

$$\hat{P}'_f(\rho) = -\frac{1}{N}\sum_{i=1}^{N}\phi_h(g(\mathbf{x}_i,\rho))g'(\mathbf{x}_i,\rho). \tag{2.10}$$

2.3. **Common Random Variable Approach.** The Common Random Variable (CRV) approach can also be employed when the design parameter ρ does not affect the distribution $f_{\mathbf{x}}$. In this case, we take the central Finite Difference approximation [3, 34]

$$\overline{P}'_f(\rho) = \frac{P_f(\rho+\tau) - P_f(\rho-\tau)}{2\tau}, \tag{2.11}$$

where the same sample is used to estimate both $P_f(\rho+\tau)$ and $P_f(\rho-\tau)$ [19], with τ used to denote the step size. This measure is known to reduce the variance of the estimate in comparison to direct employment of Finite Difference formulas, as demonstrated in [44]. The MCS estimate results

$$\hat{P}'_f(\rho) = \frac{\frac{1}{N}\sum_{i=1}^{N} I(g(\mathbf{x}_i, \rho+\tau)) - \frac{1}{N}\sum_{i=1}^{N} I(g(\mathbf{x}_i, \rho-\tau))}{2\tau}. \tag{2.12}$$

The CRV approach with Forward Formula was studied in [44] and is not further developed here.

3. Bias, variance and mean square error

Since MCS provides an unbiased estimate for the expected value [38], we have

$$\mathbb{E}[\hat{P}'_f(\rho)] = \overline{P}'_f(\rho), \tag{3.1}$$

for all the above approaches. The bias of the estimate $\hat{P}'_f(\rho)$ with respect to P'_f then results

$$\begin{aligned} e &= \mathbb{E}[\hat{P}'_f(\rho)] - P'_f(\rho) \\ &= \overline{P}'_f(\rho) - P'_f(\rho). \end{aligned} \tag{3.2}$$

In other words, the bias is the conceptual error of $\overline{P}'_f$ with respect to P'_f, without accounting for sampling errors. However, since sampling is a random experiment, the estimate $\hat{P}'_f$ has variance given by $\mathbb{V}[\hat{P}'_f]$. Accuracy of the estimate can then be measured by the root mean square (rms) error

$$E_{rms} = \sqrt{\mathbb{E}[(\hat{P}'_f - P'_f)^2]}. \tag{3.3}$$

In the work [44], it was demonstrated that the mean square error of the MCS estimate results

$$E^2_{rms} = e^2 + \mathbb{V}[\hat{P}'_f]. \tag{3.4}$$

Thus, in order to obtain *a priori* error estimates for the above sensitivities we need to evaluate both the bias and the variance of each approach.

3.1. **Score Function Method.** The estimate from Eq. (2.6) has expected value

$$\begin{aligned} \mathbb{E}[\hat{P}'_f] &= \frac{1}{N}\sum_{i=1}^{N} \mathbb{E}[I(g(\mathbf{x}_i, \rho))s(\mathbf{x}_i)] \\ &= \frac{1}{N}\sum_{i=1}^{N} \mathbb{E}[I(g(\mathbf{X}, \rho))s(\mathbf{X})] \\ &= P'_f. \end{aligned} \tag{3.5}$$

We thus have $e = 0$ for the Score Function Method. In other words, the Score Function Method is unbiased, since it is obtained by direct differentiation of P_f. The variance of Eq. (2.6), on the other hand, results

$$\begin{aligned}
\mathbb{V}[\hat{P}'_f] &= V[\frac{1}{N}\sum_{i=1}^{N} I(g(\mathbf{x}_i,\rho))s(\mathbf{x}_i)] \\
&= \frac{1}{N} V[I(g(\mathbf{X},\rho))s(\mathbf{X})] \\
&= \frac{1}{N}\left(\mathbb{E}[I(g(\mathbf{X},\rho))^2 s(\mathbf{X})^2] - (\mathbb{E}[I(g(\mathbf{x},\rho))s(\mathbf{X})])^2\right) \\
&= \frac{1}{N}\left(\mathbb{E}[I(g(\mathbf{X},\rho))s(\mathbf{X})^2] - (P'_f)^2\right), \qquad (3.6)
\end{aligned}$$

where we used the fact that $I(g(\mathbf{X},\rho))^2 = I(g(\mathbf{X},\rho))$.

The mean square error of the Score Function Method then results

$$E^2_{rms} = \frac{1}{N}\left(\mathbb{E}[I(g(\mathbf{X},\rho))s(\mathbf{X})^2] - (P'_f)^2\right). \qquad (3.7)$$

Note that the above error estimate is easy to employ in practice, because it requires an estimate for P'_f (that is evaluated during the procedure) and an estimate for $\mathbb{E}[I(g(\mathbf{X},\rho))s(\mathbf{X})^2]$. However, the quantity $\mathbb{E}[I(g(\mathbf{X},\rho))s(\mathbf{X})^2]$ can be estimated with the same information employed to estimate P'_f, and thus it does not require additional computational effort.

A general error estimate for the Score Function Method was previously presented in [38, 39]. This more general result holds for expectations in general (i.e. not necessarily probability of failures), derivatives of arbitrary order and consider employment of Importance Sampling. Note that MCS can be viewed as a particular case of Importance Sampling, where the sampling distribution is taken as the distribution of the random variables. For this reason, Eq. (3.7) is actually a specific purpose version of the more general result presented in [38, 39].

From Cauchy-Schwarz inequality we have

$$|\mathbb{E}[I(g(\mathbf{X},\rho))s(\mathbf{X})^2]| \leq \sqrt{\mathbb{E}[I(g(\mathbf{X},\rho))^2]\mathbb{E}[s(\mathbf{X})^4]}. \qquad (3.8)$$

Since I and s^2 are non-negative, we can write

$$\begin{aligned}
\mathbb{E}[I(g(\mathbf{X},\rho))s(\mathbf{X})^2] &\leq \sqrt{\mathbb{E}[I(g(\mathbf{X},\rho))]\mathbb{E}[s(\mathbf{X})^4]} \\
&\leq \sqrt{P_f \mathbb{E}[s(\mathbf{X})^4]}. \qquad (3.9)
\end{aligned}$$

From Cauchy-Schwarz inequality we can also write

$$\begin{aligned}
|P'_f| &= |\mathbb{E}[I(g(\mathbf{X},\rho))s(\mathbf{X})]| \\
&= |\mathbb{E}[I(g(\mathbf{X},\rho))I(g(\mathbf{X},\rho))s(\mathbf{X})]| \\
&\leq \sqrt{\mathbb{E}[I(g(\mathbf{X},\rho))]\mathbb{E}[I(g(\mathbf{X},\rho))s(\mathbf{X})^2]} \\
&\leq \sqrt{P_f \mathbb{E}[I(g(\mathbf{X},\rho))s(\mathbf{X})^2]}, \qquad (3.10)
\end{aligned}$$

that gives

$$\frac{P'^2_f}{P_f} \leq \mathbb{E}[I(g(\mathbf{X},\rho))s(\mathbf{X})^2]. \qquad (3.11)$$

From the above results we can write the lower and upper bounds as follows

$$\boxed{\frac{1}{N}\left(\frac{1}{P_f}-1\right)(P_f')^2 \leq E_{rms}^2 \leq \frac{1}{N}\left(\sqrt{P_f}\sqrt{\mathbb{E}[s(\mathbf{X})^4]}-(P_f')^2\right).} \tag{3.12}$$

It is interesting to observe that the lower bound only requires the values of P_f and P_f' and should be easier to employ in practice. Besides, even though Eq. (3.7) is a particular case of the estimates presented in [38, 39], the bounds from Eq. (3.12) are novel results.

The quantity $\mathbb{E}[s(\mathbf{X})^4]$ can be evaluated for cases of interest. For the Normal distribution with expected value μ and standard deviation σ we have, for example,

$$\mathbb{E}[s(\mathbf{X})^4] = \frac{3}{\sigma^4}, \tag{3.13}$$

when the design parameter ρ is the expected value μ. In this case, we have the bounds

$$\frac{1}{N}\left(\frac{1}{P_f}-1\right)(P_f')^2 \leq E_{rms}^2 \leq \frac{1}{N}\left(\frac{\sqrt{3P_f}}{\sigma^2}-(P_f')^2\right). \tag{3.14}$$

Derivation of specific upper bounds for other distributions involve analytical evaluation of $\mathbb{E}[s(\mathbf{X})^4]$. This subject will not be further pursued in this work.

From these results, it is important to observe that the Score Function Method with MCS has rms error proportional to $1/\sqrt{N}$ (see Eq. (3.7)). Thus, we have sub-linear convergence rate of order $1/2$. This is the same convergence rate we have for evaluation of P_f with MCS [44, 29] and the same convergence rate for MCS in general [19, 36].

3.2. **Weak Approach.** In this section, we obtain error estimates for the Weak approach in the one-dimensional case ($d = 1$). The main idea is to first demonstrate that the Weak approach is equivalent to the CRV with Central Formula for $h \to 0$. This allows employment of the bias of the Central Formula for the Weak approach, once such an equivalence rule is obtained. The resulting error estimates were found to be accurate for the general case of multidimensional random variables ($d > 1$).

From A, we know that the rectangular pulse ϕ_h can be written as

$$\phi_h(t) = -\frac{1}{h}(I(t+h/2) - I(t-h/2)). \tag{3.15}$$

In one-dimension, the sensitivity of Eq. (2.9) can then be written as

$$\overline{P}_f'(\rho) = \int_{-\infty}^{+\infty} \frac{1}{h}(I(g(x,\rho)+h/2) - I(g(x,\rho)-h/2))g'(x,\rho)f_X(x)dx. \tag{3.16}$$

We now wish to replace $g(x,\rho) \pm h/2$ by $g(x,\rho \pm \tau)$ in the above expression. In order to obtain the appropriate value for τ, consider then the first order truncated expansion

$$g(x,\rho+\tau) = g(x,\rho) + \tau g'(x,\rho). \tag{3.17}$$

From the condition

$$g(x,\rho) + h/2 = g(x,\rho+\tau), \tag{3.18}$$

we get

$$\tau(x) = \frac{h}{2g'(x,\rho)}. \tag{3.19}$$

Consequently, Eq. (3.16) can be rewritten as

$$\overline{P}'_f(\rho) = -\int_{-\infty}^{+\infty} \frac{1}{h}(I(g(x,\rho+\tau(x))) - I(g(x,\rho-\tau(x))))g'(x,\rho)f_X(x)dx, \tag{3.20}$$

with $\tau(x)$ as given above. Substitution of h from Eq. (3.19) in the above expression gives

$$\overline{P}'_f(\rho) = -\int_{-\infty}^{+\infty} \frac{1}{2\tau(x)}(I(g(x,\rho+\tau(x))) - I(g(x,\rho-\tau(x))))f_X(x)dx. \tag{3.21}$$

Let us assume that x^*, satisfying $g(x^*,\rho)=0$, is unique. Then, for $h\to 0$, the support of $I(g(x,\rho+\tau(x))) - I(g(x,\rho-\tau(x)))$ converges to x^*. By denoting

$$\tau = \tau(x^*), \tag{3.22}$$

we have, for $h\to 0$, that

$$\begin{aligned}\overline{P}'_f(\rho) &= \frac{1}{2\tau}\left[\int_{-\infty}^{+\infty} I(g(x,\rho+\tau))f_X(x)dx - \int_{-\infty}^{+\infty} I(g(x,\rho-\tau))f_X(x)dx\right] \\ &= \frac{P_f(\rho+\tau)-P_f(\rho-\tau)}{2\tau},\end{aligned} \tag{3.23}$$

which is clearly a Central Formula for the sensitivity with step size τ. This proves that, in the one-dimensional case, the Weak approach is equivalent to a Central Formula scheme for $h\to 0$ when x^* is unique. This occurs for h that satisfies Eq. (3.19) at x^*, i.e. for

$$h = 2\tau g'(x^*,\rho), \tag{3.24}$$

where τ is the step size of the central formula.

The bias of the Central Formula with step size τ is known to be given by [3, 34]

$$e = -\frac{\tau^2}{6}P'''_f(\xi),\ \xi\in[\rho-\tau,\rho+\tau]. \tag{3.25}$$

By substitution of Eq. (3.24) into the above expression, we conclude that the bias of the Weak Approach can be estimated as

$$e = -\frac{h^2}{24}\frac{P'''_f(\xi)}{(g'(x^*,\xi))^2},\ \xi\in[\rho-\tau,\rho+\tau]. \tag{3.26}$$

The variance of the Weak approach is known to be given by [44]

$$\mathbb{V}[\hat{P}'_f] = \frac{g'(x^*,\rho)P'_f(\rho)}{Nh}. \tag{3.27}$$

After taking $\xi=\rho$, the mean square error estimate becomes

$$\boxed{E^2_{rms} = \frac{h^4}{576}\frac{(P'''_f(\rho))^2}{(g'(x^*,\rho))^4} + \frac{1}{Nh}g'(x^*,\rho)P'_f(\rho).} \tag{3.28}$$

Note that this result is different from the one previously obtained in [44]. First, the procedure employed here (i.e. equivalence to a central formula) is very different from the one employed in [44]. Besides, the result now involves only derivatives of P_f and g, while the result presented in [44] also involves second order derivatives of the quantity $\psi(x^*,\rho)=g'(x^*,\rho)f_x(x^*)$ in place of $P'''_f(\rho)$. Since P'''_f is a global quantity in comparison to the point-wise quantity evaluated at x^* given by $g'(x^*,\rho)f_x(x^*)$, the result obtained here incorporates information of the problem in a

broader sense. This seems to be the reason why the estimate becomes more representative in a wider range of situations.

Even though this result was obtained in the one-dimensional case considering x^* unique, in the examples we demonstrate that it is representative for more general situations. For this reason, the above bias estimate can be viewed as an improvement over the estimate previously presented in [44].

In B we demonstrate that, in the multidimensional case, the bias can be written as

$$e = \frac{h^2}{24} \int_\Gamma \frac{\Delta\Psi(\mathbf{x})}{\|\nabla g(\mathbf{x}, \rho)\|^3} d\Gamma + o(h^2), \tag{3.29}$$

where $\mathbf{x} \in \mathbb{R}^d$ and $\Psi(\mathbf{x}) = g'(\mathbf{x}, \rho) f_{\mathbf{X}}(\mathbf{x})$, with $\Delta\Psi(\mathbf{x})$ used to denote its Laplacian with respect to $\mathbf{x}$. Finally, Γ is the hypersurface defined by $g(\mathbf{x}, \rho) = 0$. This result confirms that the bias is indeed of second order with respect to h. However, the above estimate is not efficient for computational purposes in this form, since it would require numerical integration over Γ.

3.3. **Common Random Variable (CRV) Approach.** In the work [44], the following estimate for the mean square error of the CRV approach with Central Formula was obtained

$$E_{rms}^2 = \tau^4 \frac{(P_f(\rho)''')^2}{36} + \frac{1}{N\tau} \frac{P_f'(\rho)}{2}. \tag{3.30}$$

This error estimate was found to be accurate and for this reason we do not purse other estimates for the CRV approach in this work.

3.4. **Optimal values for h and τ.** For a given sample size N, the optimal value of h for the Weak Approach can be estimated from the optimality condition

$$\frac{dE_{rms}^2}{dh} = 0. \tag{3.31}$$

This gives

$$h^5 = \frac{1}{N} \frac{144(g'(x^*, \rho))^5 P_f'(\rho)}{(P_f'''(\rho))^2}. \tag{3.32}$$

For this optimal value of h, the rms error results

$$E_{rms} = 0.6801720118 \left(\frac{P_f'(\rho) \sqrt{P_f'''(\rho)}}{N} \right)^{2/5}, \tag{3.33}$$

as can be verified by the reader[1]. This rms error is called here the "optimal error", in the sense that it is the theoretical error from optimal choice of parameter h.

Following the same procedure for the CRV with Central Formula we get

$$\tau^5 = \frac{1}{N} \frac{9 P_f'(\rho)}{2(P_f'''(\rho))^2} \tag{3.34}$$

and

[1]Note that the quantity 0.6801720118 actually corresponds to rounding of $12^{4/5}\sqrt{5}/24$.

$$E_{rms} = 0.6801720118 \left(\frac{P'_f(\rho)\sqrt{P'''_f(\rho)}}{N} \right)^{2/5}. \tag{3.35}$$

The careful reader will observe that the optimal rms error of the Weak and CRV approaches are the same. This means that both approaches will be equivalent from the convergence point of view for $N \to \infty$, as long as the optimal values for h and τ are adopted. Of course this is only a theoretical asymptoptic result, that may not hold for arbitrary values employed in practice. However, the results indicate that both approaches should have similar accuracy in practice.

Also note that for optimal h and τ, the rms error is now proportional to $1/N^{2/5}$. This indicates that both the Weak and the CRV approaches with MCS have sub-linear convergence rates of order 2/5. This convergence rate is slower than the convergence rate 1/2 of MCS for estimating P_f. Besides, it is also slower than the convergence rate of the Score Function Method with MCS. This proves that it is harder to evaluate the sensitivity with respect to design parameters that affect the limit state function than with respect to design parameters that only affect the distribution.

4. Numerical Examples

We now present some numerical examples in order to validate the *a priori* error estimates presented previously. In Section 4.1, we employ the Score Function Method to solve two examples where the design parameter only affects the distribution. In Section 4.2, we address two examples where the design parameter only affects the limit state function, that are solved with the Weak Approach and the CRV Approach with Central Formula. The rms error of the sensitivity was estimated as

$$\hat{E}_{rms} = \sqrt{\frac{1}{N_{MCS}} \sum_{i=1}^{N_{MCS}} (\hat{P}'_{fi} - P'_f)^2}, \tag{4.1}$$

where $\hat{P}_{fi}$ are sensitivity estimates, P'_f is the reference sensitivity and N_{MCS} is the number of times MCS was run in order to evaluate the rms error. In this work, we take $N_{MCS} = 100$ in all examples, since it was observed that the results do not vary significantly if N_{MCS} is further increased.

4.1. **Score Function Method.**

We first present two examples regarding sensitivity analysis when the design parameter only affects the distribution of the random variables, solved with the Score Function Method using MCS estimates. The results were obtained with samples of sizes $N = 10^3$, 10^4, 10^5 and 10^6.

4.1.1. *Roof truss.*

The first example is the roof truss previously studied in [31, 42], among others. The limit state function is given by

$$g = 0.03 - \frac{ql^2}{2}\left(\frac{3.81}{A_c E_c} + \frac{1.13}{A_s E_s}\right), \tag{4.2}$$

where q is the distributed load, l is the roof span, A_c, E_c and A_s, E_s are the cross section area and elastic modulus of the concrete and steel beams, respectively. The random variables are as described in Table 2, where CV stands for coefficient of variation [2].

[2]In Examples 4.1.1 and 4.2.1, some physical quantities which must be positive are modeled as Normal random variables. This is not recommended in practice, since negative values of these physical quantities may lead to

TABLE 2. Random variables of Example 4.1.1

Parameter	Distribution	Expected Value	CV
q (N/m)	Normal	20,000	7%
l (m)	Normal	12	1%
A_s (m^2)	Normal	9.82×10^{-4}	6%
A_c (m^2)	Normal	0.04	12%
E_s (N/m^2)	Normal	1×10^{11}	6%
E_c (N/m^2)	Normal	2×10^{10}	6%

Here we only present results of the sensitivity with respect to the expected value of A_s (i.e. $\rho = \mathbb{E}[A_s]$), since sensitivities with respect to other random variables gave similar results. The reference values for the probability of failure and its sensitivity were taken as $P_f = 0.009373$ and $P'_f = -186.262$, that are the exact values presented in [42].

The rms errors are presented in Figure 1. The rms error estimated from Eq. (4.1) associated with the numerical experiment is presented as the red dotted line. The *a priori* estimate from Eq. (3.7) is presented as the solid blue line. The bounds from Eq. (3.14) are presented as black dashed lines. From these results we observe that the estimate from Eq. (3.7) agrees very well with the rms error evaluated from numerical solutions. The bounds from Eq. (3.14) also hold, as expected.

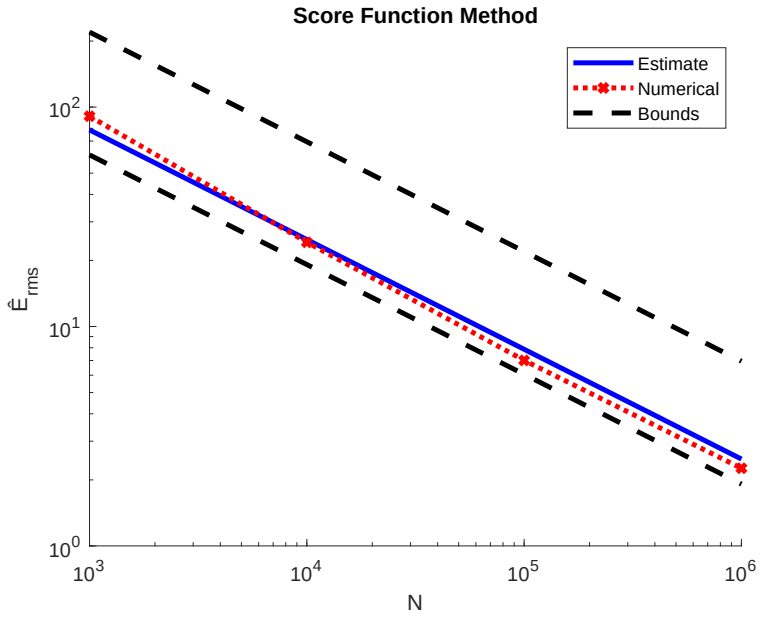

FIGURE 1. E_{rms} for Example 4.1.1

Note that the bounds are not centered. In fact, the lower bound is closer to the numerical results and the estimate. The lower bound is also easier to employ than the upper bound, since it does not require an estimate to $\mathbb{E}[s(\mathbf{X})^4]$ (see Eq. (3.12)).

spurious results. However, in this work we kept the Normal distributions originally employed in these examples in order to allow comparison to previous works. We also emphasize that the distribution was not truncated during sampling.

4.1.2. *Elastoplastic frame.* The second example is the elastoplastic frame studied in [31, 27, 53], among others. The limit state function is given by

$$g = \min\{g_1, g_2, g_3, g_4\} \tag{4.3}$$

with

$$\begin{aligned} g_1 &= 2M_1 + 2M_3 - 4.5S, \\ g_2 &= 2M_1 + M_2 + M_3 - 4.5S, \\ g_3 &= M_1 + M_2 + 2M3 - 4.5S, \\ g_4 &= M_1 + 2M_2 + M_3 - 4.5S, \end{aligned} \tag{4.4}$$

where M_i are plastic moments and S is the load magnitude. The random variables are as described in Table 3.

TABLE 3. Random variables of Example 4.1.2

Parameter	Distribution	Expected Value	CV
M_i (tm)	Lognormal	200	15%
S (tm)	Lognormal	50	40%

Here we only present results of the sensitivity with respect to the expected value of M_1 (i.e. $\rho = \mathbb{E}[M_1]$), since sensitivities with respect to other random variables gave similar results. The reference values for the probability of failure and its sensitivity were taken as $P_f = 5.29 \times 10^{-4}$ and $P'_f = -8.85 \times 10^{-6}$. These results were obtained using the Score Function Method and MCS with a sample of size 10^8 and agree with the results obtained in [31, 27]. The rms errors are presented in Figure 2. The bounds from Eq. (3.12) are presented as black dashed lines.

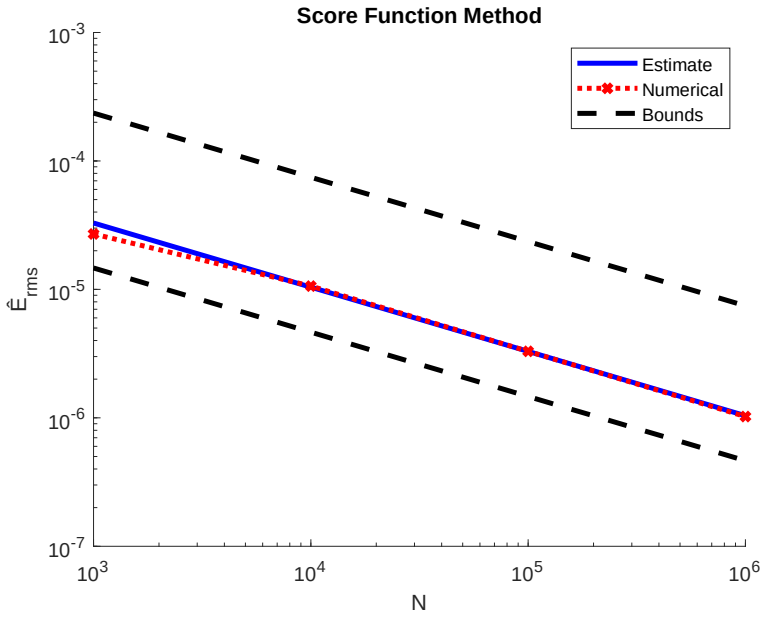

FIGURE 2. E_{rms} for Example 4.1.2

The results again agree with the estimate from Eq. (3.7) and the bounds from Eq. (3.12). Besides, the lower bounds is closer to the numerical results and the estimate again. These results seem to indicate that, in general, the lower bound may be tighter than the upper bound.

4.2. **Weak Approach and Central Formula.** We now present two examples regarding sensitivity analysis when the design parameter only affects the limit state function. These examples are solved with the Weak approach and the CRV approach with Central Formula using MCS estimates. For each sample size, the sensitivity was obtained 20 times and the mean square error with respect to a reference result was evaluated, using Eq. (4.1). The point $\mathbf{x}^*$ was taken as the most probable point of failure (MPP) obtained with the Hasofer-Lind-Rackwitz-Fiessler (HLRF) first order algorithm [28, 9, 29].

4.2.1. *Cantilever beam.* In this example, we consider the cantilever beam previously studied in [31, 49], among others. The limit state functions are given by

$$g_1 = y - \left(\frac{600}{wt^2}Y + \frac{600}{w^2t}X\right) \tag{4.5}$$

$$g_2 = D_0 - \frac{4L^3}{Ewt}\sqrt{\left(\frac{Y}{t^2}\right)^2 + \left(\frac{X}{w^2}\right)^2} \tag{4.6}$$

where y and E are the material yield stress and elastic modulus, t and w are the beam height and width, X and Y are applied loads in the direction of t and w, L is the beam length and D_0 is allowable tip displacement. The random variables are as described in Table 4.

TABLE 4. Random variables of Example 4.2.1

Parameter	Distribution	Expected Value	CV
X (lb)	Normal	500	20%
Y (lb)	Normal	1,000	10%
y (psi)	Normal	40,000	5%
E (psi)	Normal	29×10^6	5%

The results were obtained for $w = 2.4$in, $t = 3.9$in, $D_0 = 2.5$in and $L = 100$in. Here we only present results of the sensitivity with respect to t (i.e. $\rho = t$), since sensitivities with respect to other random variables gave similar results. The reference values for the probability of failure and its sensitivities were taken as $P_f = 0.00303$, $P_f' = -0.0353$ for g_1 and $P_f = 0.00025$, $P_f' = -0.00295$ for g_2, that are the values from [49]. For g_1 and g_2 the MPP is given by $x^* = \{0.069707922285513,\ 0.112127951655093,\ 3.704854131638248,\ 0.0\}\times 10^4$ and $x^* = \{0.000080221466839,\ 0.000105711272514,\ 0.0,\ 2.660714722098192\}\ \times 10^7$, respectively. The third order derivatives required by the error estimates were taken as $P_f''' = -4.17$ and $P_f''' = -0.37$ for g_1 and g_2, respectively. These results were evaluated with the CRV Approach using a third order central formula with $\tau = 0.01 \times \rho$ and $N = 10^6$. Note that a poor estimate for P_f''' may affect the accuracy of the error estimates. The values of P_f''' presented here were obtained after several computational tests. Practical implications resulting from inexact estimate of P_f''' is outside the scope of this work.

We first take the sample size $N = 10^6$. For the Central Formula we take $\tau = 3.9 \times 0.2/2^i$, $i = 0, 1, 2, ..., 15$. For the Weak Approach, we take $h = 2\tau g'(x^*, \rho)$ in order to satisfy Eq. (3.24). The rms errors obtained and the *a priori* estimate from Eq. (3.28) with respect to τ are presented in Figure 3. We observe that, for both g_1 and g_2, the error estimate agrees very well with the results. This is the main achievement of this work, since the error estimate obtained

in the work [44] was not accurate for this example. Also note that the Weak Approach and the Central Formula are equivalent for h and τ that satisfy Eq. (3.24) in this example.

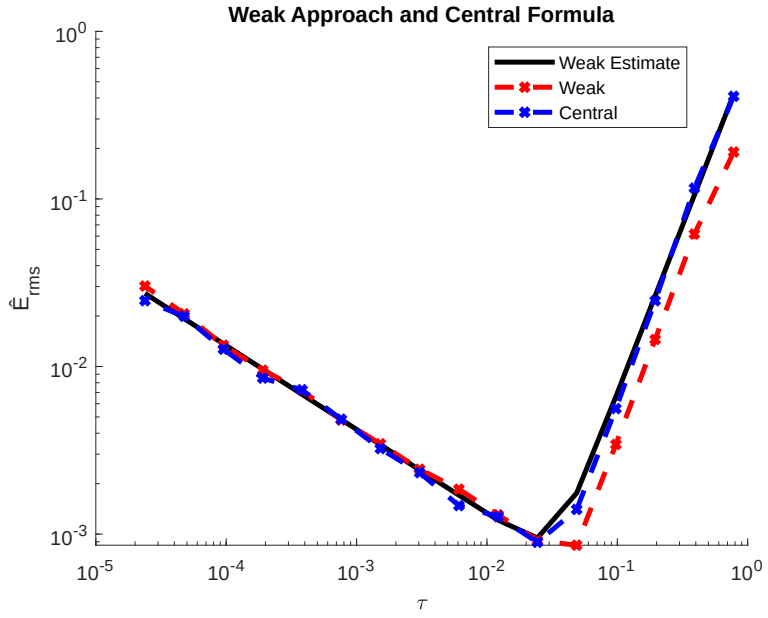

a)

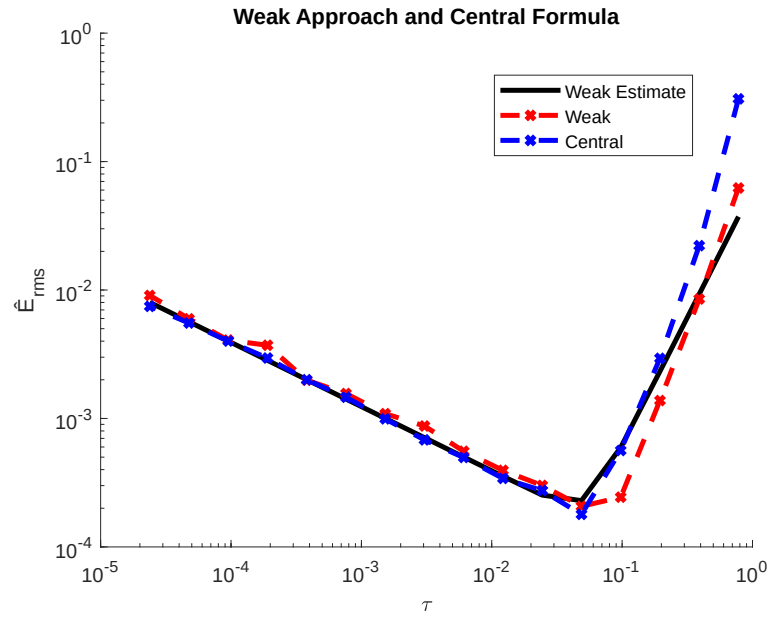

b)

FIGURE 3. E_{rms} for varying τ in Example 4.2.1 (g_1 (a) and g_2 (b))

We now take samples of sizes $N = 10^3$, 10^4, 10^5 and 10^6. The optimal parameters h and τ were evaluated with Eqs. (3.32) and (3.34). The optimal rms errors and the estimate from Eq. (3.33) with respect to N are presented in Figure 4. We observe that the results agree with the *a priori* estimate.

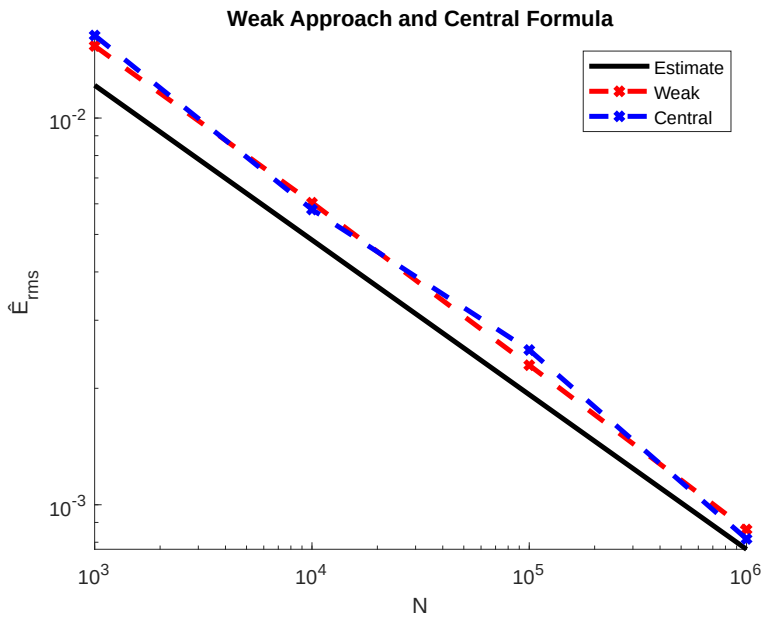

a)

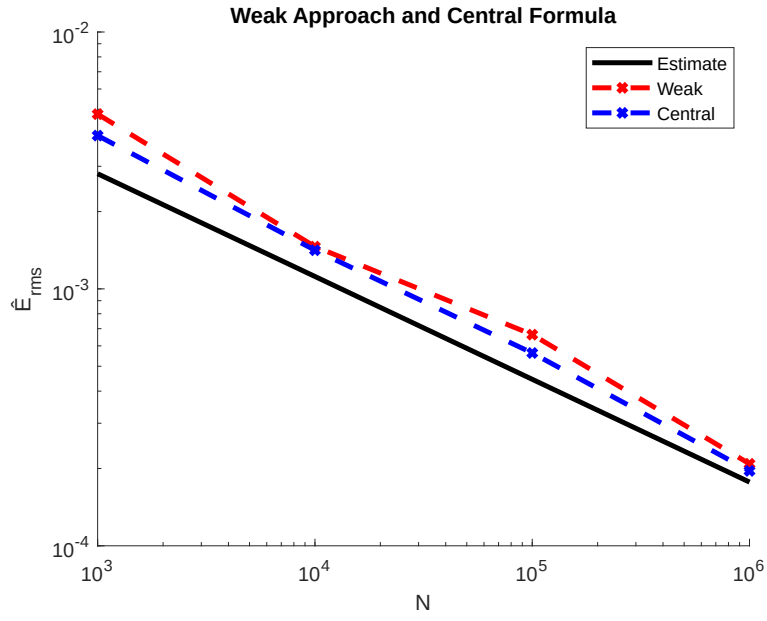

b)

FIGURE 4. E_{rms} for varying N in Example 4.2.1 (g_1 (a) and g_2 (b))

4.2.2. *Barrier problem.* In this example, we consider the probability of a Gaussian stationary stochastic process $X(t)$ surpassing a constant barrier ρ, that is also the design parameter. The stochastic processes has autocorrelation given by the exponential square law

$$\rho(t_1, t_2) = \exp\left(-\frac{(t_2 - t_1)^2}{\lambda^2}\right), \tag{4.7}$$

where λ is the correlation length. The properties of the stochastic process $X(t)$ are summarized in Table 5.

TABLE 5. Random processes from Example 4.2.2

Process	Type	Expected Value	Standard Deviation	Autocorrelation
$X(t)$	Gaussian, Stationary	$\mu = 10$	$\sigma = 2.5$	Eq. (4.7) with $\lambda = 4$

The probability of failure is defined as

$$P_f = \mathbb{P}\left[\exists a \in [0,T] | X(a) > \rho\right], \tag{4.8}$$

where $[0,T]$ is the time interval of analysis. This means that failure is assumed to occur if the barrier is surpassed by the process at some time instant.

This problem can be solved numerically by expansion of the stochastic process. Here we employ EOLE (Expansion Optimal Linear Estimation) [22]. We first assume that the time interval $[0,T]$ is divided into $k-1$ uniform time steps, defining the time instants t_1, t_2, ..., t_k. The stochastic process is then expanded as

$$X(t) = \mu(t) + \sum_{i=1}^{r} \frac{\zeta_i}{\sqrt{\theta_i}} \Phi_i^T \Sigma, \tag{4.9}$$

where $\mu(t)$ is the expected value of the process, $r < k$ is the number of terms maintained in the expansion, ζ_i are independent standard Normal random variables, Σ is the autocovariance matrix among time instants, Φ_i are the eigenvectors of Σ and θ_i its eigenvalues. The limit state function is then defined as

$$g = \max_{i=1,2,...,k} \{\rho - X(t_i)\}, \tag{4.10}$$

which assumes that failure occurs if the processes surpasses the barrier ρ at some time instant.

In this example, we consider the time interval $[0, 50]$, employ 200 uniform time steps and take the first $r = 100$ terms in the EOLE expansion. The value of the barrier is defined as the design parameter $\rho = 20$. Note that the resulting computational problem has $r = 100$ standard Normal random variables and the limit state function from Eq. (4.10) equivalent to that of a series system. Reference values were evaluated with the CRV Approach with Central Formula, using a sample of size $N = 10^7$ and $\tau = 0.2$. The results are $P_f = 0.000973$, $P_f' = -0.0015815$, $P_f'' = 0.00214$, $P_f''' = -0.0032$.

We first take $N = 10^5$ and $\tau = 20 \times 0.2/2^i$, with $i = 0, 1, 2, ..., 15$. For the Weak Approach, we take $h = 2\tau g'(x^*, \rho)$ in order to satisfy Eq. (3.24). The rms errors obtained and the *a priori* estimate from Eq. (3.28) with respect to τ are presented in Figure 5. We observe that the results agree with the *a priori* estimate.

We now take samples of sizes $N = 10^3$, 10^4, 10^5 and 10^6. The parameters h and τ were evaluated with Eqs. (3.32) and (3.34). The rms errors and the estimate from Eq. (3.33) with respect to N are presented in Figure 6. Again, the results agree with the *a priori* estimate.

5. CONCLUSIONS

In this work, *a priori* error estimates for the Score Function Method and the Weak Approach with Monte Carlo Simulation were derived, which are given respectively by Eqs. (3.12) and (3.28). The error estimate for the Weak Approach was obtained from an equivalence condition to the Finite Difference Central Formula. Even though the result was obtained in the one-dimensional case, the numerical examples indicate that it may be useful for the multidimensional context as well. An estimate for the multidimensional case was also obtained in B, which confirms that the bias is indeed of second order with respect to the parameter h.

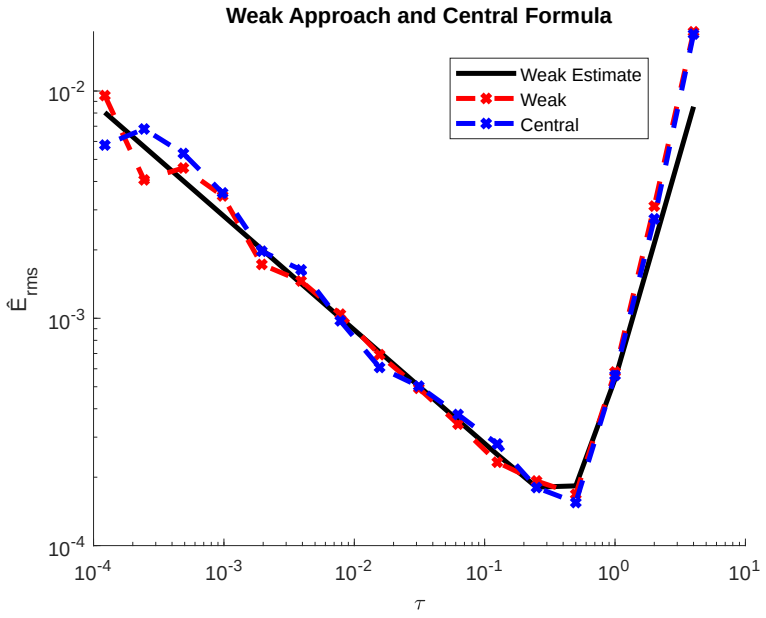

FIGURE 5. E_{rms} for varying τ in Example 4.2.2

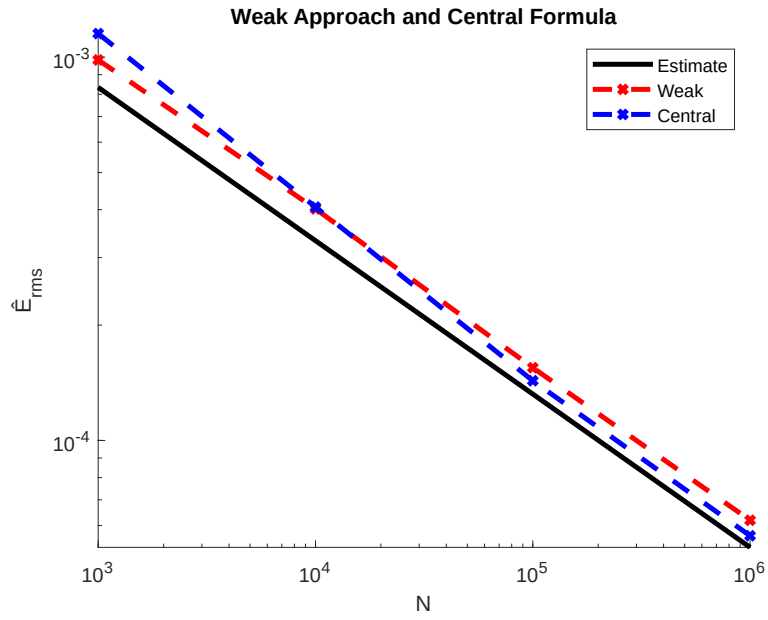

FIGURE 6. E_{rms} for varying N in Example 4.2.2

It was demonstrated that, for optimal choice of parameters, the rms error of the Weak Approach and the Common Random Variable Approach with Finite Difference Central Formula is proportional to $1/N^{2/5}$. This convergence rate is slower than that of standard Monte Carlo Simulation and the Score Function Method, which is proportional to $1/N^{1/2}$. This proves that, from the computational point of view, the sensitivity with respect to parameters that affect the

limit state function is harder to evaluate than the sensitivity with respect to parameters that only affect the distribution, as expected.

Concerning the Weak and the CRV approaches, it is important to point out that the error does not decrease monotonically as (h, τ) is reduced. In fact, for a given sample size N there exist optimal values for (h, τ), as can be seen from Figures 3 and 5. This is the same behavior observed in [44]. For (h, τ) bigger than this optimal value we have a "bias stage", where the error is dominated by the bias. For (h, τ) smaller than the optimal value, the error is dominated by the variance of the estimate and we have a "variance stage". Optimal values of the parameters are the ones that balance the bias and the variance to produce minimal error. These values lie in the transition between the bias and the variance stages.

Evaluation of the *a priori* error estimates presented here require the value of the probability of failure and its derivatives. In general, this information is unknown beforehand and cannot be evaluated exactly. Consequently, approximate values obtained with simulation may be employed for this purpose. The resulting estimates will not be exact, but may be accurate enough to evaluate the order of magnitude of the errors involved. However, we emphasize that the main goal of this work is to provide theoretical results that will contribute to a better understating of the problem and future computational advancements. For this reason, further computational aspects were not addressed here.

The results of this work are important from the conceptual point of view and can be valuable for developing *a posteriori* error estimates and adaptive sampling schemes for sensitivity analysis in the future. Finally, the error estimates presented in this work may be adapted for more advanced sampling-based schemes than standard Monte Carlo Simulation.

Acknowledgments

This research was partly supported by CNPq (Brazilian Research Council) and FAPERJ (Research Foundation of the State of Rio de Janeiro). These financial support are gratefully acknowledged.

Appendix A. Weak derivative of the indicator function I

From Figure 7, we observe that we can write

$$\begin{aligned} \phi_h(t) &= \frac{1}{h}(I(t - h/2) - I(t + h/2)) \\ &= -\frac{1}{h}(I(t + h/2) - I(t - h/2)). \end{aligned} \tag{A.1}$$

In other words, the rectangular pulse ϕ_h can be written as the central finite difference of $I(t)$ with step size $h/2$. For $h \to 0$, this leads to the well known conclusion that $\phi_h(t)$ actually represents the weak derivative of $I(t)$.

Appendix B. Results for the multidimensional case

The indicator function can be written as

$$I(t) = 1 - H(t), \tag{B.1}$$

where H is the Heaviside function. The weak derivative of I is then

$$\frac{d}{dt} I(t) = -\delta(t), \tag{B.2}$$

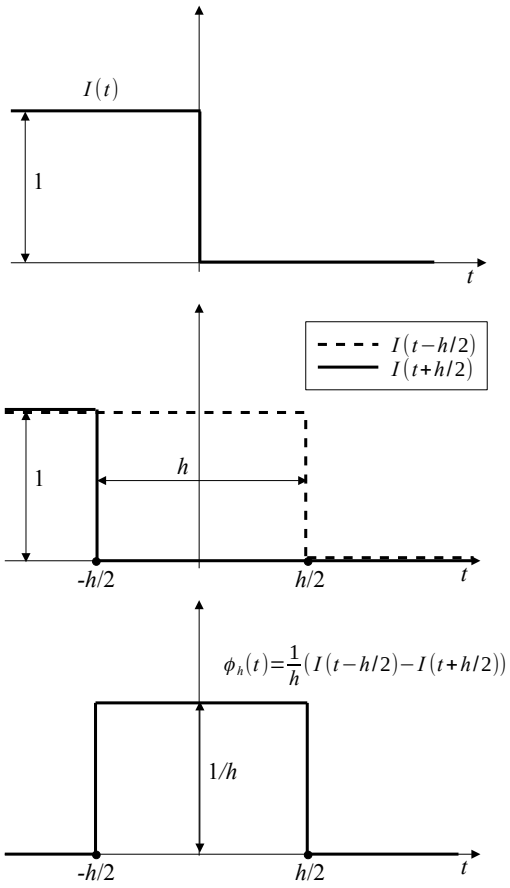

FIGURE 7. Weak Derivative

where δ is the Dirac delta function. The probability of failure sensitivity can then be written as

$$P_f'(\rho) = -\int_{\mathbb{R}^d} \delta(g(\mathbf{x},\rho)) g'(\mathbf{x},\rho) f_{\mathbf{X}}(\mathbf{x}) d\mathbf{x}. \tag{B.3}$$

The composition $\delta \circ g$ can be written as

$$\delta(g(\mathbf{x},\rho)) = \frac{\delta(\mathbf{x}-\mathbf{x}^*)}{\|\nabla g(\mathbf{x}^*,\rho)\|}, \tag{B.4}$$

provided that $g(\mathbf{x}^*,\rho) = 0$. From the coarea formula we have [16]

$$\begin{aligned} P_f'(\rho) &= -\int_{\mathbb{R}^d} \frac{\delta(\mathbf{x}-\mathbf{x}^*) g'(\mathbf{x},\rho) f_X(\mathbf{x})}{\|\nabla g(\mathbf{x}^*,\rho)\|} d\mathbf{x} \\ &= -\int_{\Gamma} \frac{g'(\mathbf{x},\rho)) f_X(\mathbf{x})}{\|\nabla g(\mathbf{x}^*,\rho)\|} d\eta(\mathbf{x}), \end{aligned} \tag{B.5}$$

where Γ is the $(d-1)$-dimensional hypersurface defined by $g(\mathbf{x}^*,\rho) = 0$ with respect to the Minkowski content measure and η is the hypersurface measure associated to Γ. Let us assume that $\mathbf{x}^*$ is unique, then

$$P'_f(\rho) = -\frac{g'(\mathbf{x}^*, \rho) f_X(\mathbf{x}^*)}{\|\nabla g(\mathbf{x}^*, \rho)\|}. \tag{B.6}$$

On the other hand, $\delta(\mathbf{x} - \mathbf{x}^*) = \delta(x_1 - x_1^*) \times \cdots \times \delta(x_d - x_d^*)$, where each $\delta(t)$ can be approximated by $\phi_\varepsilon(t)$ as follows

$$\phi_\varepsilon(t) = \begin{cases} 0, & -\infty < t \leq -\varepsilon/2 \\ 1/\varepsilon, & -\varepsilon/2 < t < \varepsilon/2 \\ 0, & +\infty > t \geq \varepsilon/2 \end{cases} \tag{B.7}$$

for $\varepsilon \to 0$. The approximated sensitivity is then given by an integral with support within the d-dimensional hypercube of size ε, namely

$$P_f^\varepsilon(\rho) = -\frac{\varepsilon^{-d}}{\|\nabla g(\mathbf{x}^*, , \rho)\|} \int_{x_d^* - \varepsilon/2}^{x_d^* + \varepsilon/2} \cdots \int_{x_1^* - \varepsilon/2}^{x_1^* + \varepsilon/2} \Psi(x_1, ..., x_d) dx_1 \cdots dx_d, \tag{B.8}$$

with $\Psi(\mathbf{x}) = g'(\mathbf{x}, \rho) f_X(\mathbf{x})$. Let us expand $\Psi(\mathbf{x})$ in Taylor series around the point $\mathbf{x}^*$ to obtain

$$\Psi(\mathbf{x}) = \Psi(\mathbf{x}^*) + \nabla\Psi(\mathbf{x}^*) \cdot (\mathbf{x} - \mathbf{x}^*) + \frac{1}{2}\nabla^2\Psi(\mathbf{x}^*)(\mathbf{x} - \mathbf{x}^*) \cdot (\mathbf{x} - \mathbf{x}^*) + \cdots, \tag{B.9}$$

which allows for solving the above integral by hand, namely

$$\begin{aligned} P_f^\varepsilon(\rho) &= -\frac{\varepsilon^{-d}}{\|\nabla g(\mathbf{x}^*, \rho)\|} \left(\varepsilon^d \Psi(\mathbf{x}^*) + \frac{\varepsilon^{2+d}}{24} \Delta\Psi(\mathbf{x}^*) \right) + o(\varepsilon^2) \\ &= -\frac{\Psi(\mathbf{x}^*)}{\|\nabla g(\mathbf{x}^*, \rho)\|} - \varepsilon^2 \frac{\Delta\Psi(\mathbf{x}^*)}{24\|\nabla g(\mathbf{x}^*, \rho)\|} + o(\varepsilon^2), \end{aligned} \tag{B.10}$$

where we have used the fact that $\nabla^2\Psi(\mathbf{x}^*) \cdot \mathbf{I} = \mathrm{tr}(\nabla^2\Psi(\mathbf{x}^*)) = \Delta\Psi(\mathbf{x}^*)$, with $\mathbf{I}$ used to denote the d-dimensional identity matrix. In the same way, $\delta(g(\mathbf{x}, \rho))$ can be approximated by $\phi_h(t)$ as

$$\phi_h(t) = \begin{cases} 0, & -\infty < t \leq -h/2 \\ 1/h, & -h/2 < t < h/2 \\ 0, & +\infty > t \geq h/2 \end{cases} \tag{B.11}$$

for $h \to 0$. Then, the following relation between ε and h holds true

$$\varepsilon = \frac{h}{\|\nabla g(\mathbf{x}^*, \rho)\|}, \tag{B.12}$$

so that the approximated sensitivity can be written in terms of the small parameter h as

$$P_f^h(\rho) = -\frac{\Psi(\mathbf{x}^*)}{\|\nabla g(\mathbf{x}^*, \rho)\|} - h^2 \frac{\Delta\Psi(\mathbf{x}^*)}{24\|\nabla g(\mathbf{x}^*, \rho)\|^3} + o(h^2) \tag{B.13}$$

Finally, the error $e^h(\mathbf{x}^*) = P'_f(\rho) - P_f^h(\rho)$ for unique $\mathbf{x}^* \in \Gamma$ is given by

$$e^h(\mathbf{x}^*) = h^2 \frac{\Delta\Psi(\mathbf{x}^*)}{24\|\nabla g(\mathbf{x}^*, \rho)\|^3} + o(h^2). \tag{B.14}$$

The bias from Eq. (B.14) was obtained for unique $\mathbf{x}^* \in \Gamma$. For this reason, Eq. (B.14) is actually a point-wise bias. However, in the general case $\mathbf{x}^* \in \Gamma$ is not unique and then the total bias is composed by the contribution of all points in Γ. This gives the bias

$$e = \int_{\Gamma} e^h(\mathbf{x}) d\Gamma, \tag{B.15}$$

that yields to

$$e = \frac{h^2}{24} \int_{\Gamma} \frac{\Delta\Psi(\mathbf{x})}{\|\nabla g(\mathbf{x}, \rho)\|^3} d\Gamma + o(h^2). \tag{B.16}$$

This result shows that the bias is indeed of second order with respect to h, as occurs in the one-dimensional case [44]. This is an important conceptual result from this work.

References

[1] Alen Alexanderian, Pierre A. Gremaud, and Ralph C. Smith. Variance-based sensitivity analysis for time-dependent processes. *Reliability Engineering & System Safety*, 196:106722, 2020.

[2] Anestis Antoniadis, Sophie Lambert-Lacroix, and Jean-Michel Poggi. Random forests for global sensitivity analysis: A selective review. *Reliability Engineering & System Safety*, 206:107312, 2021.

[3] K. E. Atkinson. *Introduction to Numerical Analysis*. John Wiley & Sons, New York, 2nd edition, 1989.

[4] S.K. Au. Reliability-based design sensitivity by efficient simulation. *Computers & Structures*, 83(14):1048 – 1061, 2005. Uncertainties in Structural Mechanics and Analysis–Computational Methods.

[5] Majdi Awad, Tristan Senga Kiesse, Zainab Assaghir, and Anne Ventura. Convergence of sensitivity analysis methods for evaluating combined influences of model inputs. *Reliability Engineering & System Safety*, 189:109 – 122, 2019.

[6] William Becker. Metafunctions for benchmarking in sensitivity analysis. *Reliability Engineering & System Safety*, 204:107189, 2020.

[7] Francesco Cadini, Simone Salvatore Lombardo, and Marco Giglio. Global reliability sensitivity analysis by sobol-based dynamic adaptive kriging importance sampling. *Structural Safety*, 87:101998, 2020.

[8] Jianbing Chen, Zhiqiang Wan, and Michael Beer. A global sensitivity index based on fréchet derivative and its efficient numerical analysis. *Probabilistic Engineering Mechanics*, 62:103096, 2020.

[9] O. Ditlevsen and H. O. Madsen. *Structural Reliability Methods*. John Wiley & Sons, Chichester, 1996.

[10] V. Dubourg and B. Sudret. Meta-model-based importance sampling for reliability sensitivity analysis. *Structural Safety*, 49:27 – 36, 2014. Special Issue In Honor of Professor Wilson H. Tang.

[11] Max Ehre, Iason Papaioannou, and Daniel Straub. A framework for global reliability sensitivity analysis in the presence of multi-uncertainty. *Reliability Engineering & System Safety*, 195:106726, 2020.

[12] Max Ehre, Iason Papaioannou, and Daniel Straub. Global sensitivity analysis in high dimensions with pls-pce. *Reliability Engineering & System Safety*, 198:106861, 2020.

[13] Wellison J. S. Gomes and André T. Beck. The design space root finding method for efficient risk optimization by simulation. *Probabilistic Engineering Mechanics*, 44:99 – 110, 2016.

[14] Qing Guo, Yongshou Liu, Bingqian Chen, and Qin Yao. A variable and mode sensitivity analysis method for structural system using a novel active learning kriging model. *Reliability Engineering & System Safety*, 206:107285, 2021.

[15] Clemens Hübler. Global sensitivity analysis for medium-dimensional structural engineering problems using stochastic collocation. *Reliability Engineering & System Safety*, 195:106749, 2020.

[16] L. Hörmander. *The Analysis of Linear Partial Differential Operators I*. Grundlehren der mathematischen Wissenschaften Book Series, vol. 256. Springer, Berlin, Heidelberg, 1983.

[17] Zdeněk Kala. Quantile-based versus sobol sensitivity analysis in limit state design. *Structures*, 28:2424 – 2430, 2020.

[18] A. N. Kolmogorov. *Foundations of the Theory of Probability*. Chelsea, New York, 1950.

[19] Dirk P. Kroese, Thomas Taimre, and Zdravko I. Botev. *Handbook of Monte Carlo Methods*. John Wiley & Sons, Hoboken, 2011.

[20] Sergei Kucherenko, Shufang Song, and Lu Wang. Quantile based global sensitivity measures. *Reliability Engineering & System Safety*, 185:35 – 48, 2019.

[21] S. Lacaze, L. Brevault, S. Missoum, and M. Balesdent. Probability of failure sensitivity with respect to decision variables. *Structural and Multidisciplinary Optimization*, 52(2):375–381, 2015.

[22] Chun-Ching Li and A. Der Kiureghian. Optimal discretization of random fields. *Journal of Engineering Mechanics*, 119(6):1136–1154, 1993.

[23] Min Li, Ruo-Qian Wang, and Gaofeng Jia. Efficient dimension reduction and surrogate-based sensitivity analysis for expensive models with high-dimensional outputs. *Reliability Engineering & System Safety*, 195:106725, 2020.

[24] Fuchao Liu, Pengfei Wei, Chenghu Tang, Pan Wang, and Zhufeng Yue. Global sensitivity analysis for multivariate outputs based on multiple response gaussian process model. *Reliability Engineering & System Safety*, 189:287 – 298, 2019.

[25] Samuele Lo Piano, Federico Ferretti, Arnald Puy, Daniel Albrecht, and Andrea Saltelli. Variance-based sensitivity analysis: The quest for better estimators and designs between explorativity and economy. *Reliability Engineering & System Safety*, 206:107300, 2021.

[26] M. Loève. *Probability Theory I*. Springer-Verlag, New York, 4th edition, 1977.

[27] Zhenzhou Lu, Shufang Song, Zhufeng Yue, and Jian Wang. Reliability sensitivity method by line sampling. *Structural Safety*, 30(6):517 – 532, 2008.

[28] H. O. Madsen, S. Krenk, and N. C. Lind. *Methods of structural safety*. Prentice Hall, Englewood Cliffs, 1986.

[29] R. E. Melchers and A. T. Beck. *Structural Reliability Analysis and Prediction*. John Wiley & Sons, Hoboken, 3rd edition, 2018.

[30] Joseph B. Nagel, Jörg Rieckermann, and Bruno Sudret. Principal component analysis and sparse polynomial chaos expansions for global sensitivity analysis and model calibration: Application to urban drainage simulation. *Reliability Engineering & System Safety*, 195:106737, 2020.

[31] Iason Papaioannou, Karl Breitung, and Daniel Straub. Reliability sensitivity estimation with sequential importance sampling. *Structural Safety*, 75:24 – 34, 2018.

[32] Carsten Proppe. Local reliability based sensitivity analysis with the moving particles method. *Reliability Engineering & System Safety*, page 107269, 2020.

[33] Gengjian Qian, Michel Massenzio, Denis Brizard, and Mohamed Ichchou. Sensitivity analysis of complex engineering systems: Approaches study and their application to vehicle restraint system crash simulation. *Reliability Engineering & System Safety*, 187:110 – 118, 2019. Sensitivity Analysis of Model Output.

[34] A. Quarteroni, R. Sacco, and F. Saleri. *Numerical Mathematics*. Springer, Berlin, 2nd edition, 2007.

[35] Sharif Rahman. Stochastic sensitivity analysis by dimensional decomposition and score functions. *Probabilistic Engineering Mechanics*, 24(3):278–287, 2009.

[36] S. M. Ross. *Simulation*. Academic Press, Orlando, 4th edition, 2006.

[37] S. M. Ross. *A First Course in Probability*. Prentice Hall, Upper Saddle River, 8th edition, 2010.

[38] R. Y. Rubinstein and D. P. Kroese. *Simulation and the Monte Carlo method*. John Wiley & Sons, Hoboken, 2nd edition, 2008.

[39] Reuven Y. Rubinstein and Alexander Shapiro. Optimization of static simulation models by the score function method. *Mathematics and Computers in Simulation*, 32(4):373–392, 1990.

[40] R.Y. Rubinstein and A. Shapiro. *Discrete event systems: sensitivity analysis and stochastic optimization by the score function method*. Wiley, Chichester, 1993.

[41] A. N. Shriryaev. *Probability*. Springer-Verlag, New York, 2nd edition, 1995.

[42] Shufang Song, Zhenzhou Lu, and Hongwei Qiao. Subset simulation for structural reliability sensitivity analysis. *Reliability Engineering & System Safety*, 94(2):658 – 665, 2009.

[43] Rui Teixeira, Alan O'Connor, and Maria Nogal. Probabilistic sensitivity analysis of offshore wind turbines using a transformed kullback-leibler divergence. *Structural Safety*, 81:101860, 2019.

[44] André Jacomel Torii. On sampling-based schemes for probability of failure sensitivity analysis. *Probabilistic Engineering Mechanics*, 62, 2020.

[45] André Jacomel Torii, R. H. Lopez, and L. F. F. Miguel. Probability of failure sensitivity analysis using polynomial expansion. *Probabilistic Engineering Mechanics*, 8:76–84, 2017.

[46] M.A. Valdebenito, H.A. Jensen, H.B. Hernández, and L. Mehrez. Sensitivity estimation of failure probability applying line sampling. *Reliability Engineering & System Safety*, 171:99 – 111, 2018.

[47] Marcos A. Valdebenito, Herman B. Hernández, and Héctor A. Jensen. Probability sensitivity estimation of linear stochastic finite element models applying line sampling. *Structural Safety*, 81:101868, 2019.

[48] Zeping Wu, Wenjie Wang, Donghui Wang, Kun Zhao, and Weihua Zhang. Global sensitivity analysis using orthogonal augmented radial basis function. *Reliability Engineering & System Safety*, 185:291 – 302, 2019.

[49] R. J. Yang and L. Gu. Experience with approximate reliability-based optimization methods. *Structural and Multidisciplinary Optimization*, 26:152–159, 2004.

[50] W Yun, Z Lu, P He, Y Dai, and K Feng. Adaptive subdomain sampling and its adaptive kriging–based method for reliability and reliability sensitivity analyses. *Structural and Multidisciplinary Optimization*, 61:1107–1121, 2020.

[51] Wanying Yun, Zhenzhou Lu, and Xian Jiang. An efficient method for moment-independent global sensitivity analysis by dimensional reduction technique and principle of maximum entropy. *Reliability Engineering & System Safety*, 187:174 – 182, 2019. Sensitivity Analysis of Model Output.

[52] Kaichao Zhang, Zhenzhou Lu, Kai Cheng, Laijun Wang, and Yanling Guo. Global sensitivity analysis for multivariate output model and dynamic models. *Reliability Engineering & System Safety*, 204:107195, 2020.

[53] Yan-Gang Zhao and Alfredo H-S. Ang. System reliability assessment by method of moments. *Journal of Structural Engineering*, 129(10):1341–1349, 2003.

[54] Di Zhou, Ershun Pan, Xufang Zhang, and Yimin Zhang. Dynamic model-based saddle-point approximation for reliability and reliability-based sensitivity analysis. *Reliability Engineering & System Safety*, 201:106972, 2020.

(A.J. Torii) Universidade Federal da Integração Latino-Americana (UNILA), Av. Tancredo Neves 6731, Foz do Iguaçu, 85867-970, Brazil

Email address: andre.torii@unila.edu.br

(A.A. Novotny) Laboratório Nacional de Computação Científica LNCC/MCTI, Coordenação de Métodos Matemáticos e Computacionais,, Av. Getúlio Vargas 333, 25651-075 Petrópolis - RJ, Brasil

Email address: novotny@lncc.br